

## **Targeted Mutagenesis of the ALS-Linked FUS protein to determine the specific cellular effects of the P525L and P525R mutations.**

Rosanna Garris  
Department of Chemistry  
The University of North Carolina Asheville  
One University Heights  
Asheville, North Carolina, 28804 USA

Faculty Advisor: Angel Kaur

### **Abstract**

Amyotrophic Lateral Sclerosis (ALS) is a rare neurodegenerative disease that involves protein-aggregate formation, axonal retreat, and death of motor neurons. Despite many individual genes and gene mutations found to be common across ALS patients, the underlying cause and disease promoting cellular mechanisms are unknown. Mutations in one of these proteins, Fused in Sarcoma (FUS), have been found to account for 4% of familial ALS cases. The two mutations of interest are FUS-P525L, a highly prevalent mutation in aggressive cases of juvenile onset ALS, and a novel ALS-related mutant, FUS-P525R, which is at the same position and has shown similar effects. The functional impact of these mutations has not been well studied, but mutations in this region are known to cause the protein to mislocalize from the nucleus to the cytoplasm. Once in the cytoplasm, mutant FUS is available to interact with many other proteins, resulting in the creation of degradation resistant protein aggregates that accumulate in the cell. This research involves creating the FUS P525L and FUS P525R mutations for expression in a neuronal cell line to study resulting protein aggregates, viability, and functionality of an ‘infected’ cell. The FUS P525L mutation was created and transfected into HEK 293 cells for assaying.

### **1. Introduction**

Amyotrophic lateral sclerosis (ALS) is a rare adult-onset neurodegenerative disease characterized by dendritic altering, axonal retreat and eventual death of affected neurons, primarily motor neurons.<sup>1,2</sup> Though the prevalence is low, 1 in every 20,000 people, the chance an individual will contract the disease increases as an individual ages.<sup>1</sup> Disease onset generally occurs between the ages of 56 and 70, and has a slightly increased prevalence in men.<sup>1</sup> Death results, after a median time of 36 months from symptom onset, due to respiratory failure.<sup>3</sup>

Clinical symptoms of ALS include the loss of muscle control, often beginning in the extremities and gradually spreading to the rest of the body. ALS can be sub-classified by multiple markers: location of onset, disease focality, presence of cognitive defects, age of onset, life span, and heritability.<sup>1</sup> Though primarily characterized by motor neuron loss, ALS is often co-diagnosed with Frontotemporal Dementia (FTD), a disorder resulting in the degeneration of the neurons in the frontal and temporal lobes by what appears to be a similar mechanism.<sup>3</sup> Onset can be bulbar or spinal, and focality can be in either the upper or lower neurons, or in any of the extremities. The locality and focality of the disease tend to be indicative of prognosis.<sup>1</sup> ALS can also be classified as familial (fALS) or sporadic (sALS). These relate to the prevalence of the disease in one’s lineage, with only 10% of ALS cases being heritable and thus classified as fALS.<sup>1</sup>

ALS results in denervation of the neuromuscular junction (NMJ) via axonal retreat from the synapse.<sup>4</sup> This does not follow the normal Wallerian denervation typical of normal aging and nerve damage. Instead, it more closely resembles the axonal retrieval that occurs during synaptic development and refinement.<sup>4</sup> The exact cause of this retreat is unknown, however in the case of one of the many mutation-prone proteins associated with ALS, SOD1, some mutations lead to decreased mitochondrial function, leading to lowered  $\text{Ca}^{2+}$  at the synapse.<sup>4</sup> This would lead to

decreased NT release and lowered postsynaptic response, possibly making the connection less effective, therefore signaling for depotentiation and synaptic breakdown.

As of yet, no single mutation has been definitively identified as the disease trigger. Instead, the cause of ALS is considered to be a class of mutation prone proteins that work in conjunction with environmental triggers to alter cellular function in a similar way, leading to denervation and cell death. There are multiple hypothesized mechanisms for ALS development which are thought to be dependent on the specific protein mutations. However, one of the unifying features across clinically diverse ALS cases as characterized thus far, is the “prion-like” spread of the disease. True prions are misfolded proteins that are capable of spreading not only from cell to cell, but also between organisms.<sup>5</sup> In the case of ALS, the misfolded proteins are not transmissible between organisms. These misfolded proteins can form cytotoxic inclusions that are thought to travel to other cells and induce misfolding in other, “healthy” proteins. It is for this reason that it is considered a “prion-like” disease propagation as opposed to that found in a true prion disease. Over 25 different genes have been found to have mutations associated with ALS.<sup>1,3,6</sup> The majority of these proteins function as transcription factors, chaperone proteins or are somehow involved in protein regulation and turnover.<sup>6</sup> The majority of these proteins contain low-sequence complexity domains (LSCD) that allow them to interact with multiple targets, but also make them prone to misfolding.<sup>6</sup>

The specific focus of this research is mutations in the FUS (fused in sarcoma) protein. FUS mutations account for 4-5% of fALS cases and are associated with a relatively young age of disease onset (20s-30s) and shorter life expectancy, with 85% of patients dying within three years of symptom onset.<sup>3,7,8</sup> Though the incidence of these mutations is low, the fact that they can promote early onset sets them apart from other ALS-associated proteins. Over 50% of the ALS associated FUS mutations occur at the C-terminal end and disrupt appropriate cellular localization of the protein.<sup>8,9</sup> During healthy functioning, FUS is involved in multiple RNA related functions, acting as a transcription factor and playing a role in alternative splicing and oxidative stress repair.<sup>9,10,11,12</sup>

C-terminal mutations disrupt the nuclear localization sequence and cause the protein to mislocalize in the cytoplasm, where it can no longer carry out its normal function. Despite this, knockout studies investigating the role loss of oxidative repair function may play in ALS pathology have found that the loss of FUS does not significantly affect cell survivability and only slightly affects cell proliferation.<sup>9</sup> However, because oxidative damage has been linked to neurodegeneration, it is possible that the loss of function may be necessary for further mutations to occur, leading to disease onset.<sup>1,7</sup> The exact mechanism by which these inclusions may contribute to cell death is unknown. This is because multiple cellular effects have been observed in FUS-mutated ALS. This supports the hypothesis that the mechanism of cell death in ALS is due to something other than loss of the mutated proteins’ function and may be specific to the specific mutations present.

FUS is capable of performing many cellular tasks with little specificity due to its LSCDs. These domains allow FUS to interact with multiple other proteins, RNA and DNA.<sup>13</sup> Disease pathology has been linked to the interactions of FUS with cytoplasmic protein complexes known as stress granules. In healthy cells, stress granules form to bind and protect mRNA in response to environmental stress so they are not altered or degraded.<sup>5</sup> This is a cellular mechanism that is utilized to create membraneless cellular subcompartments, including stress granules. Because FUS normally resides in the nucleus, it cannot interact with these proteins. However, due to mutations that alter the protein’s localization, FUS is able to interact with these SGs in an irreversible mechanism, leading to liquid-to-solid transitions.<sup>5</sup> When FUS is recruited by a SG, it leads to a liquid-to-solid transition of the entire complex, thus increasing the stiffness and viscosity of the SG.<sup>13</sup> This complex can then become resistant to cellular degradation, and therefore altering cellular function. The accumulation of these SGs in neurons throughout an individual’s lifetime alters other cellular functions and could contribute to cell death.<sup>13</sup> After a certain portion of neuronal cell death, symptom onset occurs.

A specific mutation, R495X, has been linked to decreased mitochondrial length. This nonsense mutation leads to a premature stop codon that not only causes FUS to reside in the cytoplasm, but also causes it to inhibit the translation of mitochondria associated proteins, leading to mitochondrial shortening and decreased activity.<sup>11</sup> There is also research to support that other FUS mutants can cause translational issues of intra-axonal proteins, including the ion pumps necessary for axonal firing.<sup>14</sup> FUS mutations have also been linked to an upregulation of the nonsense-mediated decay (NMD) pathway, the pathway that is responsible for degrading mRNA with nonsense mutations in the cytoplasm.<sup>15</sup> Because of the large array of cellular effects that have been observed with FUS-positive aggregates, research regarding the exact cellular effects of specific mutations are necessary to understand commonalities that lead to prion-like formations and disease spread, and the distinctions that lead to the vast prognostic differences.

The mutations of interest, FUS P525L and P525R are aggressive mutations associated with juvenile onset (20s-30s).<sup>3</sup> Though both of these mutations are rare, their aggressive nature (death within 18-36 months of symptom onset) makes them ideal for investigation within the proposed model system.<sup>3</sup> The presence of aggressive, early onset symptoms implies high rates of cell death early in an individual’s life, suggesting there may be a large change in

cellular conditions, structure and/or viability in assays conducted. This is supported by a case study where an individual with the FUS P525R mutation developed an aggressive form of ALS while carrying no other of the known ALS- associated mutations.<sup>16</sup> Most of the research regarding these mutants has been in the form of case studies, where scientists observed clinical progression and genetic markers of the disease.<sup>16</sup> While these studies lay the foundation for understanding the prevalence and clinical presentation of this mutant type, the cellular mechanism by which this mutant is so aggressive remains unknown.

This lab primarily looks at the cellular effects of mutations on two ALS-associated proteins, TDP-43 and FUS. FUS accounts for 4% of fALS cases.<sup>3</sup> This research involves the creation of a library of FUS-mutants through targeted mutagenesis in a bacterial vector containing the Fus sequence, and subsequent subcloning into a mammalian vector plasmid (Flexi A12). Once this vector is co-transfected into mammalian cells, either HEK 293 or NSC-34, with its regulatory vector (Neo) expression levels can be modulated to ensure WT transfection does not induce aggregation. These transfected cells will be analyzed for relative RNA and protein concentrations, neurite structure and cell viability. This model system, which enables us to investigate the amount of aggregation specifically induced by the mutation, will allow us to better understand the amounts of aggregation formed by mutations as well as possible downstream effects.

## 2. Methods

### 2.1 Bacterial Vector Preparation

#### 2.1.1 Mutagenesis

Polymerized chain reaction (PCR) primers for the desired mutant were designed for the Fus sequence (HsCD00513161) using NEBasechanger (<https://nebasechanger.neb.com/>). 25-50  $\mu$ L PCR reactions were created using Q5 Hotstart High Fidelity 2X Master Mix (NEB, M0494S), each primer to a final concentration of 0.5  $\mu$ M and between 1-25 ng of template DNA. Reactions were run through 35 cycles at different annealing temperatures, dependent on the mutant, as recommended by NEBasechanger. PCR product was purified using the Invitrogen PCR Clean up kit (Thermo Fisher Scientific, K310002).

#### 2.1.2 Ligation and Transformation

Linear DNA from the PCR was then circularized using KLD treatment (NEB, M0554S) and incubated at room temperature for 5 minutes. Finally, the circular vectors were biotransformed into competent NEB-85 *E. coli* cells. After incubation, between 30-70  $\mu$ L of cells were spread onto LB-SPEC plates (100 $\mu$ g/mL spectinomycin) and allowed to grow at 37.0 °C for approximately 36 hours.

#### 2.1.3 Plasmid Preparation

Colonies were harvested and incubated at 37.0 °C with shaking in 2 mL of LB-SPEC (100  $\mu$ g/mL) for 13-15 hours. Plasmids were then prepared using the Purelink Miniprep kit (Thermo Fisher Scientific, K210010). DNA concentrations were quantified using nanodrop and sequenced via Sanger Sequencing.

### 2.2 Mammalian Vector Preparation

#### 2.2.1 Addition of Restriction Sites

Reactions we set up to contain 200  $\mu$ M dNTPs, 2  $\mu$ M of both the forward and reverse primers designed to include desired restriction sites. Reactions were run through the following protocol in a thermocycler: 98°C for 3 minutes, 34 cycles of 98°C for 10 seconds, X°C for 30 seconds (where X= annealing temperature as determined by NEB) , 72°C for 50 seconds, and a final 10 minute 72°C stage before being held at 4°C indefinitely. Samples were then run on a 1.2% agarose gel and purified using the Invitrogen Gel and PCR Clean-up Kit (Thermo Fisher Scientific, K310002).

## 2.2.2 *Restriction Digest*

PmeI and Sgfl co-digest were set up for PCR products from the previous step containing desired mutation, and for vector recipient (Flexi 12A). Reactions (50 $\mu$ L) were initially set up to contain 2  $\mu$ g or 1  $\mu$ g of DNA, respectively, 10X CutSmart Buffer to a 1X concentration, and 10 units of both enzymes and filled to volume with nuclease-free water. These were then incubated at 37 °C for 20 minutes. The recipient vector reaction was heat inactivated at 65 °C for 20 minutes. Mutant DNA underwent PCR clean up (Thermo Fisher Scientific, K310002)

## 2.2.3 *Vector Ligation*

The ligation of 50 ng of recipient DNA and 37.5 ng of insert DNA was conducted in 20  $\mu$ L reaction containing 1  $\mu$ L of T4 DNA ligase and T4 ligase buffer to a 1x concentration. These reactions were incubated at 16 °C for 16 hours before the enzyme was heat inactivated at 65 °C for 10 minutes.

## 2.2.4 *Biotransformation*

Ligate was added to NEB-85 competent E. coli cells and incubated on ice for 30 minutes. The cells were then heat shocked at 42 °C for 45 seconds and placed back on ice for 2 minutes before 900  $\mu$ L of SOC medium was added and the tubes were placed in a shaking incubator at 37 °C and 230 rpm for 1 hour. Cells were pelletized by centrifugation at 9000xg for 3 minutes. Supernatant was then removed to approximately 100  $\mu$ L and the pellet resuspended. These cells were then plated on LB-agar-KAN plates and incubated at 37 °C for 12-16 hours.

## 2.2.5 *Plasmid Preparation*

Colonies were harvested and incubated at 37.0 °C with shaking in 2 mL of LB-KAN (100  $\mu$ g/mL) for 13-15 hours. Plasmids were then prepared using the purelink miniprep kit (Thermo Fisher Scientific, K210010). DNA concentrations were then quantified using a Nanodrop and sequenced via Sanger Sequencing.

## 2.3 Transfection and Mammalian Culture

### 2.3.1 *Cell proliferation*

HEK 293 and NSC-34 cells were proliferated from cryostock into Delbecco's Modified Eagle Medium (DMEM) with ten percent fetal bovine serum (FBS). Cells were perpetuated via 1:10 splits every 2-3 days, or upon confluence.

### 2.3.2 *Cell differentiation*

NSC-34 cells were differentiated into motor-neuron like cells in proliferation media composed of 1:1 DMEM: Ham's F12 plus 1 % FBS and 1 % Penicillin/Streptomycin and 1 % Modified Eagle Medium- Non-essential amino acid solution.

### 2.3.3 *Transfection*

Transfection was conducted one day after splitting for HEK 293 cells or differentiation for NSC-34 cells when cells were 75-90 % confluence. For each well in a 12 well plate, 125  $\mu$ L of Optimem and 5  $\mu$ L of Lipofectamine 2000 was combined and incubated at room temperature for 5 minutes, a total of 2 ug of DNA was then added and allowed to incubate for 20 min at room temperature. Flexi-A12, Neo and GFP vectors were added in a 1:1:2 ratio unless otherwise indicated on the plate map. 250  $\mu$ L of the Opti/DNA/Lipo mixture was added dropwise to the well and rocked to mix. Coumermycin was dosed on cells at desired concentration at the time of transfection. Cells were allowed to incubate overnight at 37.0 °C and 5% CO<sub>2</sub>, medium was replaced the following morning. Cells then incubated for another 48 hours before experiments were run.

### 3. Results and Discussion

#### 3.1 Bacterial Vector Amplification and Conformation

##### 3.1.1 *FUS P525L*

Mutant carrying bacterial vectors were created and grown in accordance with the described methods. Figure 1 shows the successful colony grown with the mutated *FUS* vector. The vector was extracted and submitted for sanger sequencing which confirmed the presence of the desired *FUS* mutant within the vector sequence. Normally, hundreds of colonies are present on the plates, however, this particular mutant grew much less successfully than other mutants being created. It was determined that, due to the location of the mutant in the *FUS* sequence, the primers designed for mutagenesis were initially not accounting for the sequence of the vector at the end of the protein encoding sequence. It is likely that because of this, insufficient quantities of the complete vector with the desired mutation were being produced during the initial mutagenesis process, causing a lower success rate during the ligation and bacterial transformation steps.



Figure 1. The bacterial colony from which *FUS P525L* bacterial vector was harvested.

##### 3.1.2 *FUS P525R*

The creation of the *FUS P525R* mutation was attempted utilizing the same protocols. However, the mutant could never be successfully biotransformed. In fact, the PCR mutagenesis yielded either multiple different length segments of DNA or no reaction occurred. Despite altering annealing temperature, elongation periods and DNA quantity in turn the mutation could not be successfully created in the given timeframe.

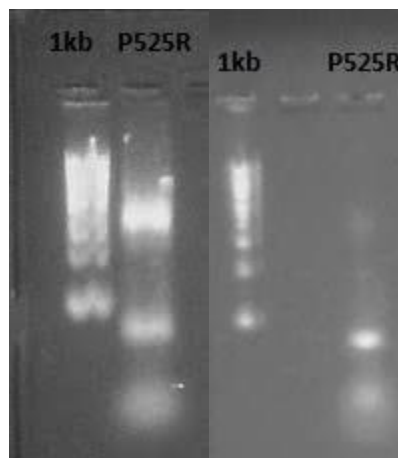


Figure 2. Agarose gels comparison.

Figure 2 Two attempts to create the FUS P525R mutation using the same protocol. The agarose gel on the left shows a blurred, band, likely spanning many lengths of DNA. The right-hand gel yielded no DNA at or around the proper length.

### 3.2 Mammalian Vector Preparation

#### 3.2.1 FUS P525L

Mammalian vectors were prepared in accordance with the protocol previously described. Figure 2 shows the successful subcloning of the FUS P525L mutation ligated into a vector. Representative colonies underwent colony PCR and successful colonies were cultured for DNA extraction. DNA was submitted for sanger sequencing which yielded a single successful mutant.

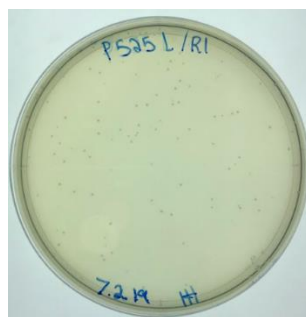


Figure 3. Bacterial colonies containing the FUS P525L mammalian vector.

#### 3.2.2 other mammalian mutants created.

In conjunction with the primary mutations of interest, other mutations were created in the mammalian vector using the same methodology (Table 1).

Table 1. Other FUS and TDP-43 subcloned into the Flexi vector.

Protein and mutation	Blast Sequence Alignment			
FUS TG ins (1420-1422 TG insertion)	Query 1403	ACGGGGATGATCGTCGTGGTG	--GCAGAGGAGGCTATGATCGAGGCGGCTACCGGGCG	1460
	Sbjct 516	ACGGGGATGATCGTCGTGGTG	GGCAGAGGAGGCTATGATCGAGGCGGCTACCGGGCG	575
TDP-43 A382T (1144 G to A)	Query 1102	GGTTCTGGAAATAACTCTTATAGTGGCTCTAATTCTGGTGCAGCAATTGGTTGGGATCA	1161	
	Sbjct 395	GGTTCTGGAAATAACTCTTATAGTGGCTCTAATTCTGGTGCACAAATTGGTTGGGATCA		454
TDP-43 I383V (1147 A to G)	Query 1102	GGTTCTGGAAATAACTCTTATAGTGGCTCTAATTCTGGTGCAGCAATTGGTTGGGATCA	1161	
	Sbjct 397	GGTTCTGGAAATAACTCTTATAGTGGCTCTAATTCTGGTGCAGCAGTTGGTTGGGATCA		456

### 3.3 Mammalian Culture and Transfection

HEK 293 cells were cultured and transfected according to the described protocol. Initially, to confirm transfection protocols, only EGFP was transfected, Figure X shows the successful transfection with cells expressing the vector indicated. After this assay a larger assay was undertaken to establish the baseline level of expression desired. Flexi-FUS P525L and Flexi-FUS were tested in triplicate at coumermycin concentrations of 0, 2.5, 5.0, and 10.0 nanomolar. These were run along with a media only, EGFP and Neo vector only controls, also done in triplicate at each concentration (Table 2).

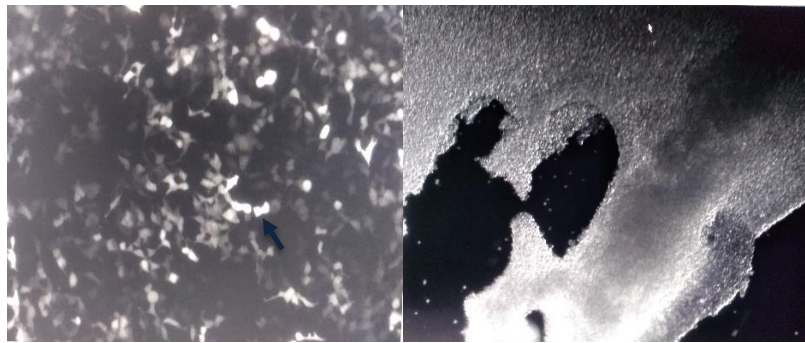


Figure 4. HEK 293 cells post-transfection.

Figure 4 The left-hand panel shows the first attempt a transfection with only EGFP. Indicated are glowing cells which were successfully transfected (40X magnification). The right-hand panel shows cell folding that was observed in the second transfection attempt (10X magnification).

As can be seen in figure 4, transfection was equally successful. However, the cells do not appear to have remained adherent, and therefore they were not viable for further analysis. It is known that the HEK 293 cell line is prone to loss of adherence phenotype after multiple replication cycles.<sup>17</sup> It is possible that the cells being used had mutated and therefore lost the ability to adhere, making them inappropriate for further analysis.

Table 2. Description of samples transfected.

10.0 nM couermycin	5.0 nM couermycin	2.5 nM couermycin	0.0 nM couermycin
Media only	Media only	Media only	Media only
0.25 µg EGFP	0.25 µg EGFP	0.25 µg EGFP	0.25 µg EGFP
0.25 µg EGFP 0.25 µg Neo	0.25 µg EGFP 0.25 µg Neo	0.25 µg EGFP 0.25 µg Neo	0.25 µg EGFP 0.25 µg Neo
0.25 µg EGFP 0.25 µg Neo 0.25 µg FUS	0.25 µg EGFP 0.25 µg Neo 0.25 µg FUS	0.25 µg EGF 0.25 µg Neo 0.25 µg FUS	0.25 µg EGFP 0.25 µg Neo 0.25 µg FUS
0.25 µg EGF 0.25 µg Neo 0.25 µg FUS P525L	0.25 µg EGFP 0.25 µg Neo 0.25 µg FUS P525L	0.25 µg EGFP 0.25 µg Neo 0.25 µg FUS P525L	0.25 µg EGFP 0.25 µg Neo 0.25 µg FUS P525L

#### 4. Conclusions

The vector system utilized in this research, will allow for better understanding of the specific effects of the aggregates these mutations form. By regulating the expression of the target protein, we can ensure that aggregation is not occurring due to overexpression of the transfected protein, but due to its mutation. This will allow for the specific effects of the aggregates to be analyzed. Though the particular mutations of interest were not successfully created, methodologies were created and modified that allowed for the successful creation of mutations in both FUS and TDP-43 proteins. These methodologies can be used to create subsequent mutations to prepare for analysis and the created mutants can be transfected into various cell lines for analysis.

#### 5. Acknowledgements

The author wishes to acknowledge Angel Kaur for her guidance and advise throughout this project as well as Thomas Meigs for his support and assistance with mammalian culture. The author also wished to acknowledge her lab partner Hannah Henken, for her support and collaboration as well as the other members of the Kaur lab.

## 6. References

1. Martin, S; Al Khleifat, A.; Al-Chalabi, A. What causes amyotrophic lateral sclerosis? *F1000Research*. **2017** 6, 371.
2. Fogarty, M.J.; Mu, E.W.H.; Lavidis, N.A.; Noakes, P.G.; Bellingham, M.C. Motor Areas Show Altered Dendritic Structure in an Amyotrophic Lateral Sclerosis Mouse Model. *Front. Neurosci.* **2017**, 11, 609.
3. Corcia, P., Couratier, P.; Blasco, H.; Andres, C. R.; Beltran, S.; Meininger, V.; Vourc'h, P. Genetics of amyotrophic lateral sclerosis. *Revue Neurologique*. **2017** 173, 254-262.
4. Arbour, D., Veldé, C. V.; Robitaille, R. New perspectives on amyotrophic lateral sclerosis: the role of glial cells at the neuromuscular junction. *J. Physiol.* **2017** 595, 647–661.
5. Brauer, S.; Zimyanin, V.; Hermann, A. Prion-like properties of disease-relevant proteins in amyotrophic lateral sclerosis. *J. Neural. Transm. (Vienna)*. **2017** 125, 591-613.
6. Mao Y.; Kuo S-W.; Chen L.; Heckman CJ.; Jiang M.C. The essential and downstream common proteins of amyotrophic lateral sclerosis: A protein-protein interaction network analysis. *PLOS ONE*. **2017** 12, 3.
7. Millecamps, S.; Salachas, F.; Cazeneuve, C.; Gordan, P.; Brücka, B.; Camuzat, A.; Guillot-Noël, L.; Russaouen, O.; Bruneteau, G.; Pradat, P. F., et al. SOD1, ANG, VAPB, TARDBP, and FUS mutations in familial amyotrophic lateral sclerosis: genotype-phenotype correlations. *J. Med. Genet.* **2010** 47, 554-60.
8. Lattante, S. Rouleau, G.A.; Kabashi, E. TARDBP and FUS mutations associated with amyotrophic lateral sclerosis: summary and update. *Hum Mutat.* **2013** 34, 812-26.
9. Wang, H.; Guo, W.; Mitra, J. et al. Mutant FUS causes DNA ligation defects to inhibit oxidative damage repair in Amyotrophic Lateral Sclerosis. *Nature Communications*. **2018** 9, 3683.
10. Jiang, X.; Zhang, T.; Wang, H.; Wang, T.; Qin, M.; Bao, P.; Wang, R.; Liu, Y.; Chang, H.C.; Yan, J.; Xu, J. Neurodegeneration-associated FUS is a novel regulator of circadian gene expression. *Translational Neurodegeneration*. **2018**, 7, 24.
11. Nakaya, T.; Marakakis, M. Amyotrophic Lateral Sclerosis associated FUS mutation shortens mitochondria and induces neurotoxicity. *Scientific Reports*. **2018** 8, 15575.
12. Kapeli, K.; Pratt, G.A.; Vu, A.Q.; Hutt, K.R.; Martinez, F. J.; Sundararaman, B.; Batra, R.; Freese, P.; Lambert, N.J.; Huela, S.C.; Chun, S.J.; Liang, T.Y.; Chang, J.; Donohue, J.P.; Shiue, L.; Shang, J.; Zhu, H.; Cambi, F.; Kararskis, E.; Hoon, S.; Ares, M.; Burge, C.B.; Ravits, J.; Rigo, F.; Yeo, G.W. Distinct and shared functions of ALS-associated proteins TDP-43, FUS and TAF15 revealed by multisystem analyses. *Nat. Commun.* **2016** 7, 12143.
13. Antonacci, G.; de Turris, V.; Rosa, V.; Ruocco, G. Background-deflection Brillouin microscopy reveals altered biomechanics of intracellular stress granules by ALS protein FUS. *Communications Biology*. **2018** 1, 139.
14. Lopez-Erauskin, J.; Tadokoro, T.; Baughn, M.W.; Myers, B.; McAlonis-Downes, M.; Chillon-Marinas, C.; Asiaban, J.N.; Artates, J.; Bui, A.T.; Vetto, A.P.; Lee, S.K.; Le, A.V.; Sun, Y.; Jambeau, M.; Boubaker, J.; Swing, D.; Qui, J.; Hicks, G.G.; Ouyang, Z.; Fu, X.D.; Tessarolle, L.; Ling, S.C.; Parone, P.A.; Shaw, C.E.; Marsala, M.; Lagier-Tourenne, C.; Cleveland, D.W.; Da Cruz, S. ALS/FTD-linked mutation in FUS suppresses intra-axonal protein synthesis and drives disease without nuclear loss-of-function in FUS. *Neuron*. **2018** 100, 816-830.
15. Kamelgarn, M.; Chen, J.; Kuang, L.; Jin, H.; Kasarkis, E. J.; Zhu, H. ALS mutations of FUS suppress protein translation and disrupt the regulation of nonsense-mediated decay. *PNAS*. **2018** 10, 1073.
16. Kuang, L.; Kamelgarn, M.; Arenas, A.; Gal, J.; Taylor, D.; Gong, W.; Brown, M.; St. Clair, D.; Kasarskis, E.J.; Zhu, H. Clinical and experimental studies of a novel P525R FUS mutation in amyotrophic lateral sclerosis. *Neurol Genet*. **2017**, 3, e172.
17. Yao-Cheg, L.; Boone, M.; Meuris, L.; Lemmens, I.; Van Roy, N.; Soete, A.; Reumers, J.; Moisse, M.; Plaisance, S.; Drmanca, R.; Chen, J.; Speleman, F.; Lambrechts, D.; Van de Peer, Y.; Tavernier, J.; Callewaert, N. Genomic dynamics of the human embryonic kidney 293 lineage in response to cell biology manipulations. *Nature Communications*. **2014**, 4767, 5, 4767.